

String Theory at LHC Using Supersymmetry Production From String Balls

Gouranga C. Nayak^{1,*}

¹ *22 West Fourth Street #1, Lewistown, Pennsylvania 17044, USA*

(Dated: October 28, 2018)

Abstract

If extra dimensions are found in the second run of LHC in the pp collisions at $\sqrt{s} = 14$ TeV then the string scale can be \sim TeV, and we should produce string balls at LHC. In this paper we study supersymmetry (squark and gluino) production from string balls at LHC in pp collisions at $\sqrt{s} = 14$ TeV and compare that with the parton fusion results using pQCD. We find significant squark and gluino production from string balls at LHC which is comparable to parton fusion pQCD results. Hence, in the absence of black hole production at LHC, an enhancement in supersymmetry production can be a signature of TeV scale string physics at LHC.

PACS numbers: 11.25.Wx; 11.25.Db; 14.80.Ly; 12.60.Jv

*Electronic address: nayak@max2.physics.sunysb.edu

I. INTRODUCTION

The large hadron collider (LHC) has completed its first run where we have not found any evidence of the beyond standard model physics in pp collisions at $\sqrt{s} = 7$ TeV and 8 TeV respectively [1]. The LHC has started its second run involving pp collisions at $\sqrt{s} = 13$ TeV and will reach its maximum energy $\sqrt{s} = 14$ TeV in pp collisions in future. Hence all our calculations in this paper is performed at the maximum energy in the pp collisions at the LHC, *i. e.*, in pp collisions at $\sqrt{s} = 14$ TeV. The LHC will also collide two lead nuclei at $\sqrt{s} = 5.5$ TeV per nucleon to produce quark-gluon plasma [2, 3]. Since the total energy in the two lead nuclei collisions at LHC will be ~ 1150 TeV, we may expect to see new physics [4] in the nuclear collisions at LHC as well.

If we find extra dimensions in the second run at LHC in the pp collisions at $\sqrt{s} = 14$ TeV then the scale of quantum gravity *could be* as low as \sim TeV [5–22]. In the presence of extra dimensions, the string mass scale M_s and the Planck mass M_P could be around \sim TeV. In this situation we can look forward to search for TeV scale string physics at CERN LHC. Also, it is unknown if supersymmetry is manifested in nature, and if SUSY does exist it is unclear at what energy scale SUSY becomes manifest. Note that, as mentioned above, we have not found any experimental evidence for string ball production and supersymmetry production in the first run at LHC [1]. Hence, we can only search for string balls, extra dimensions and superpartners in the second run at the LHC. If we manage to detect *any* of these exotic phenomena, then we will be propelled into the twenty-first century, as our understanding of quantum gravity and perhaps even string theory is revolutionized.

One of the most exciting possibility is to search for TeV scale black hole and string ball production at LHC. These ‘brane-world’ black holes and string balls will be our first window into the extra dimensions of space predicted by string theory, and required by the several brane-world scenarios [23]. There may be many other ways of testing string theory at LHC starting from brane excitations to various string excitations. The string balls of [24] is just one such model, where the predictions are done in a toy string theory model. In this paper we will focus on studying string theory at LHC based on string balls.

There has been arguments that the black hole stops radiating near Planck scale and forms a black hole remnant [25]. These black hole remnants can be a source of dark matter [26, 27]. In the absence of a theory of quantum gravity, we can study other scenarios of black

hole emissions near the Planck scale. Ultimately, experimental data will determine which scenarios are valid near the Planck scale. In this paper we will study string ball production at LHC in the context of black hole evaporation in string theory. Recently, string theory has given convincing microscopic calculation for black hole evaporation [28, 29].

String theory predicts that a black hole has formed at several times the Planck scale and any thing smaller will dissolve into some thing known as string ball [24]. A string ball is a highly excited long string which emits massless (and massive) particles at Hagedorn temperature with thermal spectrum [30, 31]. For general relativistic description of the black hole to be valid, the black hole mass M_{BH} has to be larger than the Planck mass M_P . In string theory the string ball mass M_{SB} is larger than the string mass scale M_s . Typically

$$\begin{aligned} M_s &< M_P < \frac{M_s}{g_s^2} \\ M_s &\ll M_{SB} \ll \frac{M_s}{g_s^2} \\ \frac{M_s}{g_s^2} &\ll M_{BH} \end{aligned} \tag{1}$$

where g_s is the string coupling which can be less than 1 for the string perturbation theory to be valid. Since string ball is lighter than black hole, more string balls are expected to be produced at CERN LHC than black holes.

The Hagedorn temperature of a string ball is given by

$$T_{SB} = \frac{M_s}{\sqrt{8\pi}} \tag{2}$$

where $M_s \sim \text{TeV}$ is the string scale. Since this temperature is very high at LHC (\sim hundreds of GeV) we expect more massive particles ($M \sim 3T_{SB}$) to be produced at CERN LHC from string balls.

In this paper we study squark and gluino production from string balls at CERN LHC and make a comparison with the squark and gluino production from the parton fusion processes using pQCD. We present the results for the total cross section, rapidity distribution and $\frac{d\sigma}{dp_T}$ of squark and gluino production. There can be significant squark and gluino production from black holes at LHC as well [32]. This is because the black hole temperature increases as its mass decreases whereas the string ball temperature remains constant (see eq. (2)). On the other hand the string ball mass is smaller than the black hole mass and more string balls are produced at LHC. Hence squark and gluino production at LHC is from two

competitive effects: 1) string ball (black hole) production at LHC and 2) squark and gluino emission from a single string ball (black hole) at LHC. We find significant squark and gluino production from string balls at LHC. Hence, in the absence of black hole production at LHC, an enhancement in the supersymmetry production may be a signature of TeV scale string physics at LHC.

The paper is organized as follows. In section II we discuss string balls in string theory. In section III we describe squark and gluino production in pQCD. Section IV describes squark and gluino production from string balls at the CERN LHC. We present our results and discussions in section V and conclude in section VI.

II. STRING BALLS IN STRING THEORY

In string theory the fundamental scales are as follows: l_P is the Planck length scale, l_s is the quantum length scale of the string, $\alpha' = l_s^2$ is the inverse of the classical string tension, $M_s = \frac{1}{l_s}$ is the string mass scale and g_s is the string coupling. In small string coupling

$$l_P \sim g_s l_s. \quad (3)$$

For $d = 3 + n$ space dimensions one obtains

$$l_P^{d-1} \sim g_s^2 l_s^{d-1}. \quad (4)$$

As black hole shrinks it reaches the correspondence point [28, 29]

$$M \leq M_c \sim \frac{M_s}{g_s^2} \quad (5)$$

and makes a transition to a configuration dominated by a highly excited long string (known as string ball) which continues to lose mass by evaporation at the Hagedorn temperature [30] and "puffs-up" to a larger "random-walk" size which has observational consequences. Evaporation, still at the Hagedorn temperature, then gradually brings the size of the string ball down towards l_s .

At LHC we are interested in production and decay of highly excited string. Production of a highly excited string from the collision of two light string states at high \sqrt{s} can be obtained from the Virasoro-Shapiro four point amplitude

$$A(s, t) = \frac{2\pi g_s^2 \Gamma[-1 - \alpha' s/4] \Gamma[-1 - \alpha' t/4] \Gamma[-1 - \alpha' u/4]}{\Gamma[2 + \alpha' s/4] \Gamma[2 + \alpha' t/4] \Gamma[2 + \alpha' u/4]} \quad (6)$$

by using string perturbation theory with

$$s + t + u = -16/\alpha'. \quad (7)$$

The production cross section is therefore given by

$$\sigma \sim \frac{\pi \text{Res} A(\alpha' s/4 = N, t = 0)}{s} = g_s^2 \frac{\pi^2}{8} \alpha'^2 s. \quad (8)$$

The cross section in eq. (8) saturates the unitarity bounds at around $g_s^2 \alpha' s \sim 1$ which implies that the production cross section for string balls grows with s as in eq. (8) only for

$$M_s \ll \sqrt{s} \ll M_s/g_s, \quad (9)$$

while for

$$\sqrt{s} \gg M_s/g_s, \quad \sigma_{SB} = \frac{1}{M_s^2} \quad (10)$$

which is constant.

The string ball production cross section in a parton-parton collision is therefore given by [24]

$$\begin{aligned} \hat{\sigma}_{SB} &\sim \frac{g_s^2 M_{SB}^2}{M_s^4}, & M_s \ll M_{SB} \ll M_s/g_s, \\ \hat{\sigma}_{SB} &\sim \frac{1}{M_s^2}, & M_s/g_s \ll M_{SB} \ll M_s/g_s^2. \end{aligned} \quad (11)$$

Highly excited long strings emit massless (and massive) particles at Hagedorn temperature as given by eq. (2) by using the conventional description of evaporation in terms of black body radiation [30] where the emission can take place either in the bulk (in to the closed string) or in the brane (in to open strings).

III. SQUARK AND GLUINO PRODUCTION IN PP COLLISIONS AT LHC USING PQCD

In this section we discuss the supersymmetry (squark and gluino) production in quark and gluon fusion processes using pQCD methods applied to high energy hadronic collisions. The leading order (LO) Feynman diagrams are given in Fig. 1.

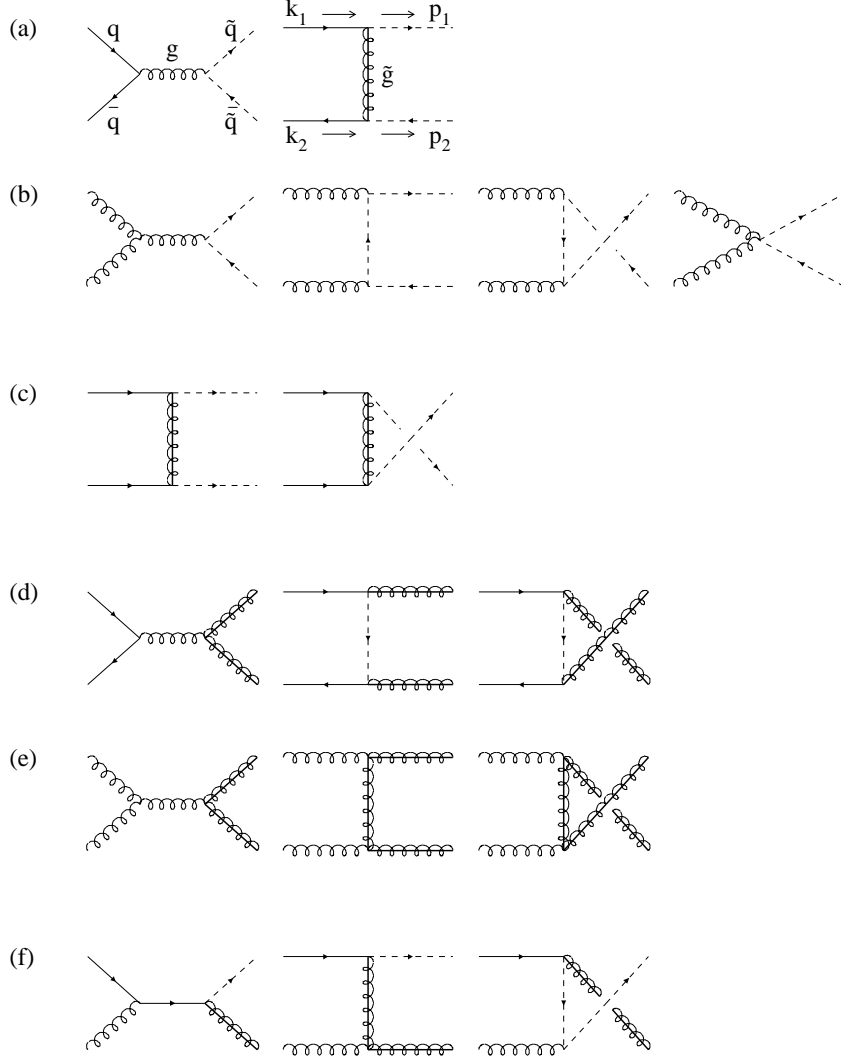


FIG. 1: Feynman diagrams for the production of squarks and gluinos in lowest order.

The differential cross section in the lowest order (LO) is given by:

$$\frac{d\sigma}{dp_t^2 dy} = \frac{H}{s} \sum_{i,j=q,\bar{q},g} \int_{x_1^{min}}^1 dx_1 \left(-\frac{1}{x_1^2 t} \right) f_{i/A}(x_1, p_t^2) f_{j/B}\left(-\frac{x_1 ts}{x_1 s + u}, p_t^2\right) \times \sum |M|^2\left(\frac{-x_1^2 ts}{x_1 s + u}, x_1 t, -\frac{x_1 tu}{x_1 s + u}\right) \quad (12)$$

where s is the total center of mass energy at hadronic level, $t = -\sqrt{s(p_t^2 + m^2)} e^y$ and $u = -\sqrt{s(p_t^2 + m^2)} e^{-y}$ where the lower limit of the x_1 integration is given by $x_1^{min} =$

$-u/s + t$. In the above equation $f_{i/p}(x, Q^2)$ is the parton distribution function inside a proton with longitudinal momentum fraction x and factorization scale Q , $H = K_{ij}/16\pi$ with $K_{q\bar{q}} = K_{q\bar{q}} = 1/36$, $K_{gg} = 1/256$ and $K_{qg} = 1/96$.

The matrix element squares from partonic fusion processes at the Born level (see Fig-1) are given by [33]:

$$\begin{aligned}
\sum |\mathcal{M}^B|^2(q_i \bar{q}_j \rightarrow \tilde{q} \tilde{q}) &= \delta_{ij} \left[32n_f g_s^4 \frac{\hat{t}_q \hat{u}_q - m_{\tilde{q}}^2 \hat{s}}{\hat{s}^2} + 16\hat{g}_s^4 \frac{\hat{t}_q \hat{u}_q - (m_{\tilde{q}}^2 - m_{\tilde{g}}^2) \hat{s}}{\hat{t}_g^2} \right. \\
&\quad \left. - 32/3 g_s^2 \hat{g}_s^2 \frac{\hat{t}_q \hat{u}_q - m_{\tilde{q}}^2 \hat{s}}{\hat{s} \hat{t}_g} \right] + (1 - \delta_{ij}) \left[16\hat{g}_s^4 \frac{\hat{t}_q \hat{u}_q - (m_{\tilde{q}}^2 - m_{\tilde{g}}^2) \hat{s}}{\hat{t}_g^2} \right] \\
\sum |\mathcal{M}^B|^2(gg \rightarrow \tilde{q} \tilde{q}) &= 4n_f g_s^4 \left[24 \left(1 - 2 \frac{\hat{t}_q \hat{u}_q}{\hat{s}^2} \right) - 8/3 \right] \left[1 - 2 \frac{\hat{s} m_{\tilde{q}}^2}{\hat{t}_q \hat{u}_q} \left(1 - \frac{\hat{s} m_{\tilde{q}}^2}{\hat{t}_q \hat{u}_q} \right) \right] \\
\sum |\mathcal{M}^B|^2(q_i q_j \rightarrow \tilde{q} \tilde{q}) &= \delta_{ij} \left[8\hat{g}_s^4 (\hat{t}_q \hat{u}_q - m_{\tilde{q}}^2 \hat{s}) \left(\frac{1}{\hat{t}_g^2} + \frac{1}{\hat{u}_g^2} \right) \right. \\
&\quad \left. + 16\hat{g}_s^4 m_{\tilde{g}}^2 \hat{s} \left(\left(\frac{1}{\hat{t}_g^2} + \frac{1}{\hat{u}_g^2} \right) - 8/3 \frac{1}{\hat{t}_g \hat{u}_g} \right) \right] \\
&\quad + (1 - \delta_{ij}) \left[16\hat{g}_s^4 \frac{\hat{t}_q \hat{u}_q - (m_{\tilde{q}}^2 - m_{\tilde{g}}^2) \hat{s}}{\hat{t}_g^2} \right] \\
\sum |\mathcal{M}^B|^2(q\bar{q} \rightarrow \tilde{g} \tilde{g}) &= 96g_s^4 \left[\frac{2m_{\tilde{g}}^2 \hat{s} + \hat{t}_g^2 + \hat{u}_g^2}{\hat{s}^2} \right] \\
&\quad + 96g_s^2 \hat{g}_s^2 \left[\frac{m_{\tilde{g}}^2 \hat{s} + \hat{t}_g^2}{\hat{s} \hat{t}_q} + \frac{m_{\tilde{g}}^2 \hat{s} + \hat{u}_g^2}{\hat{s} \hat{u}_q} \right] \\
&\quad + 2\hat{g}_s^4 \left[24 \left(\frac{\hat{t}_g^2}{\hat{t}_q^2} + \frac{\hat{u}_g^2}{\hat{u}_q^2} \right) + 8/3 \left(2 \frac{m_{\tilde{g}}^2 \hat{s}}{\hat{t}_q \hat{u}_q} - \frac{\hat{t}_g^2}{\hat{t}_q^2} - \frac{\hat{u}_g^2}{\hat{u}_q^2} \right) \right] \\
\sum |\mathcal{M}^B|^2(gg \rightarrow \tilde{g} \tilde{g}) &= 576g_s^4 \left(1 - \frac{\hat{t}_g \hat{u}_g}{\hat{s}^2} \right) \left[\frac{\hat{s}^2}{\hat{t}_g \hat{u}_g} - 2 + 4 \frac{m_{\tilde{g}}^2 \hat{s}}{\hat{t}_g \hat{u}_g} \left(1 - \frac{m_{\tilde{g}}^2 \hat{s}}{\hat{t}_g \hat{u}_g} \right) \right] \\
\sum |\mathcal{M}^B|^2(qg \rightarrow \tilde{q} \tilde{g}) &= 2g_s^2 \hat{g}_s^2 \left[24 \left(1 - 2 \frac{\hat{s} \hat{u}_q}{\hat{t}_g^2} \right) - 8/3 \right] \left[-\frac{\hat{t}_g}{\hat{s}} \right. \\
&\quad \left. + \frac{2(m_{\tilde{g}}^2 - m_{\tilde{q}}^2) \hat{t}_g}{\hat{s} \hat{u}_q} \left(1 + \frac{m_{\tilde{q}}^2}{\hat{u}_q} + \frac{m_{\tilde{g}}^2}{\hat{t}_g} \right) \right],
\end{aligned}$$

where the variables $\hat{t}_{q,g}$ ($\hat{u}_{q,g}$) are related to the Mandelstam variables \hat{t} (\hat{u}) by: \hat{t}_q (\hat{u}_q) = \hat{t} (\hat{u}) - $m_{\tilde{q}}^2$ and \hat{t}_g (\hat{u}_g) = \hat{t} (\hat{u}) - $m_{\tilde{g}}^2$ where $m_{\tilde{q}}$ ($m_{\tilde{g}}$) is the mass of the squark (gluino). The g_s is the QCD gauge coupling (qqg) and \hat{g}_s is the Yukawa coupling ($q\tilde{q}\tilde{g}$), n_f is the number of flavors and

$$\hat{s} = -\frac{x_1^2 ts}{x_1 s + u} \quad \hat{t}_{g(q)} = x_1 t \quad \hat{u}_{g(q)} = -\frac{x_1 tu}{x_1 s + u}. \quad (13)$$

The p_t differential cross sections for squarks and gluinos at LHC are determined from the above formula by integrating over the rapidity:

$$\frac{d\sigma}{dp_t} = 2p_t \int_{-\cosh^{-1}(\frac{\sqrt{s}}{2(\sqrt{p_t^2+m^2}})}^{\cosh^{-1}(\frac{\sqrt{s}}{2(\sqrt{p_t^2+m^2}})} dy \frac{d\sigma}{dm_t^2 dy} \quad (14)$$

and the rapidity differential cross sections for squarks and gluinos produced at LHC are given by integrating over p_t :

$$\frac{d\sigma}{dy} = \int_{m^2}^{s/4\cosh^2 y} dm_t^2 \frac{d\sigma}{dm_t^2 dy}. \quad (15)$$

Squark Production From String Balls at LHC

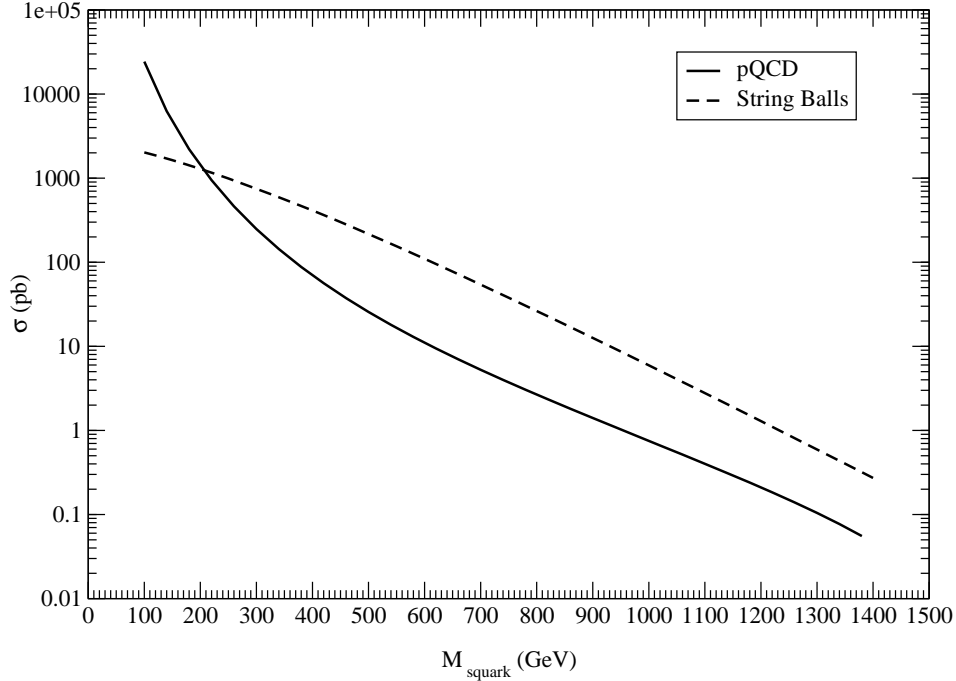


FIG. 2: Total cross section for squark production at LHC as a function of squark mass.

Similarly the total cross sections for squarks and gluinos produced at LHC are then given by:

$$\sigma^{pp \rightarrow \tilde{q}\tilde{q}(\tilde{g}\tilde{g})} = \Sigma_{i,j} \int_{4M^2/s} dx_1 \int_{4m^2/sx_1} dx_2 f_{i/p}(x_1, Q^2) f_{j/p}(x_2, Q^2) \sigma^{ij}(\hat{s}) \quad (16)$$

where σ^{ij} is the partonic level cross section for the collisions $ij \rightarrow \tilde{q}\tilde{q}(\tilde{g}\tilde{g})$ etc., where the indices i, j run over q, \bar{q} and g . The partonic level center of mass energy \hat{s} is related to the hadronic level center of mass energy s by: $\hat{s} = x_1 x_2 s$ and the partonic level squark and

gluino production cross sections $\sigma^{ij}(\hat{s})$ can be obtained from the matrix element squares above and are given by:

$$\begin{aligned}
\sigma^B(q_i \bar{q}_j \rightarrow \tilde{q} \tilde{\bar{q}}) &= \delta_{ij} \frac{n_f \pi \alpha_s^2}{\hat{s}} \beta_{\tilde{q}} \left[\frac{4}{27} - \frac{16m_{\tilde{q}}^2}{27\hat{s}} \right] \\
&\quad + \delta_{ij} \frac{\pi \alpha_s \hat{\alpha}_s}{\hat{s}} \left[\beta_{\tilde{q}} \left(\frac{4}{27} + \frac{8m_-^2}{27\hat{s}} \right) + \left(\frac{8m_{\tilde{g}}^2}{27\hat{s}} + \frac{8m_-^4}{27\hat{s}^2} \right) \log \left(\frac{\hat{s} + 2m_-^2 - \hat{s}\beta_{\tilde{q}}}{\hat{s} + 2m_-^2 + \hat{s}\beta_{\tilde{q}}} \right) \right] \\
&\quad + \frac{\pi \hat{\alpha}_s^2}{\hat{s}} \left[\beta_{\tilde{q}} \left(-\frac{4}{9} - \frac{4m_-^4}{9(m_{\tilde{g}}^2 \hat{s} + m_-^4)} \right) + \left(-\frac{4}{9} - \frac{8m_-^2}{9\hat{s}} \right) \log \left(\frac{\hat{s} + 2m_-^2 - \hat{s}\beta_{\tilde{q}}}{\hat{s} + 2m_-^2 + \hat{s}\beta_{\tilde{q}}} \right) \right] \\
\sigma^B(gg \rightarrow \tilde{q} \tilde{\bar{q}}) &= \frac{n_f \pi \alpha_s^2}{\hat{s}} \left[\beta_{\tilde{q}} \left(\frac{5}{24} + \frac{31m_{\tilde{q}}^2}{12\hat{s}} \right) + \left(\frac{4m_{\tilde{q}}^2}{3\hat{s}} + \frac{m_{\tilde{q}}^4}{3\hat{s}^2} \right) \log \left(\frac{1 - \beta_{\tilde{q}}}{1 + \beta_{\tilde{q}}} \right) \right] \\
\sigma^B(q_i q_j \rightarrow \tilde{q} \tilde{q}) &= \frac{\pi \hat{\alpha}_s^2}{\hat{s}} \left[\beta_{\tilde{q}} \left(-\frac{4}{9} - \frac{4m_-^4}{9(m_{\tilde{g}}^2 \hat{s} + m_-^4)} \right) + \left(-\frac{4}{9} - \frac{8m_-^2}{9\hat{s}} \right) \log \left(\frac{\hat{s} + 2m_-^2 - \hat{s}\beta_{\tilde{q}}}{\hat{s} + 2m_-^2 + \hat{s}\beta_{\tilde{q}}} \right) \right] \\
&\quad + \delta_{ij} \frac{\pi \hat{\alpha}_s^2}{\hat{s}} \left[\frac{8m_{\tilde{g}}^2}{27(\hat{s} + 2m_-^2)} \log \left(\frac{\hat{s} + 2m_-^2 - \hat{s}\beta_{\tilde{q}}}{\hat{s} + 2m_-^2 + \hat{s}\beta_{\tilde{q}}} \right) \right] \\
\sigma^B(q\bar{q} \rightarrow \tilde{g} \tilde{g}) &= \frac{\pi \alpha_s^2}{\hat{s}} \beta_{\tilde{g}} \left(\frac{8}{9} + \frac{16m_{\tilde{g}}^2}{9\hat{s}} \right) \\
&\quad + \frac{\pi \alpha_s \hat{\alpha}_s}{\hat{s}} \left[\beta_{\tilde{g}} \left(-\frac{4}{3} - \frac{8m_-^2}{3\hat{s}} \right) + \left(\frac{8m_{\tilde{g}}^2}{3\hat{s}} + \frac{8m_-^4}{3\hat{s}^2} \right) \log \left(\frac{\hat{s} - 2m_-^2 - \hat{s}\beta_{\tilde{g}}}{\hat{s} - 2m_-^2 + \hat{s}\beta_{\tilde{g}}} \right) \right] \\
&\quad + \frac{\pi \hat{\alpha}_s^2}{\hat{s}} \left[\beta_{\tilde{g}} \left(\frac{32}{27} + \frac{32m_-^4}{27(m_{\tilde{g}}^2 \hat{s} + m_-^4)} \right) + \left(-\frac{64m_-^2}{27\hat{s}} - \frac{8m_{\tilde{g}}^2}{27(\hat{s} - 2m_-^2)} \right) \log \left(\frac{\hat{s} - 2m_-^2 - \hat{s}\beta_{\tilde{g}}}{\hat{s} - 2m_-^2 + \hat{s}\beta_{\tilde{g}}} \right) \right] \\
\sigma^B(gg \rightarrow \tilde{g} \tilde{g}) &= \frac{\pi \alpha_s^2}{\hat{s}} \left[\beta_{\tilde{g}} \left(-3 - \frac{51m_{\tilde{g}}^2}{4\hat{s}} \right) + \left(-\frac{9}{4} - \frac{9m_{\tilde{g}}^2}{\hat{s}} + \frac{9m_{\tilde{g}}^4}{\hat{s}^2} \right) \log \left(\frac{1 - \beta_{\tilde{g}}}{1 + \beta_{\tilde{g}}} \right) \right] \\
\sigma^B(qg \rightarrow \tilde{q} \tilde{g}) &= \frac{\pi \alpha_s \hat{\alpha}_s}{\hat{s}} \left[\frac{\kappa}{\hat{s}} \left(-\frac{7}{9} - \frac{32m_-^2}{9\hat{s}} \right) + \left(-\frac{8m_-^2}{9\hat{s}} + \frac{2m_{\tilde{q}}^2 m_-^2}{\hat{s}^2} + \frac{8m_-^4}{9\hat{s}^2} \right) \log \left(\frac{\hat{s} - m_-^2 - \kappa}{\hat{s} - m_-^2 + \kappa} \right) \right. \\
&\quad \left. + \left(-1 - \frac{2m_-^2}{\hat{s}} + \frac{2m_{\tilde{q}}^2 m_-^2}{\hat{s}^2} \right) \log \left(\frac{\hat{s} + m_-^2 - \kappa}{\hat{s} + m_-^2 + \kappa} \right) \right],
\end{aligned}$$

with

$$\beta_{\tilde{q}} = \sqrt{1 - \frac{4m_{\tilde{q}}^2}{\hat{s}}} \quad \beta_{\tilde{g}} = \sqrt{1 - \frac{4m_{\tilde{g}}^2}{\hat{s}}} \quad (17)$$

$$m_-^2 = m_{\tilde{g}}^2 - m_{\tilde{q}}^2 \quad \kappa = \sqrt{(\hat{s} - m_{\tilde{g}}^2 - m_{\tilde{q}}^2)^2 - 4m_{\tilde{g}}^2 m_{\tilde{q}}^2} \quad (18)$$

$$\alpha_s = g_s^2/4\pi \quad \hat{\alpha}_s = \hat{g}_s^2/4\pi. \quad (19)$$

In our calculation we set the strong coupling equal to the QCD-SUSY coupling: $g_s = \hat{g}_s$ and use the CTEQ6M PDF inside the proton [34]. We choose the factorization and

Gluino Production From String Balls at LHC

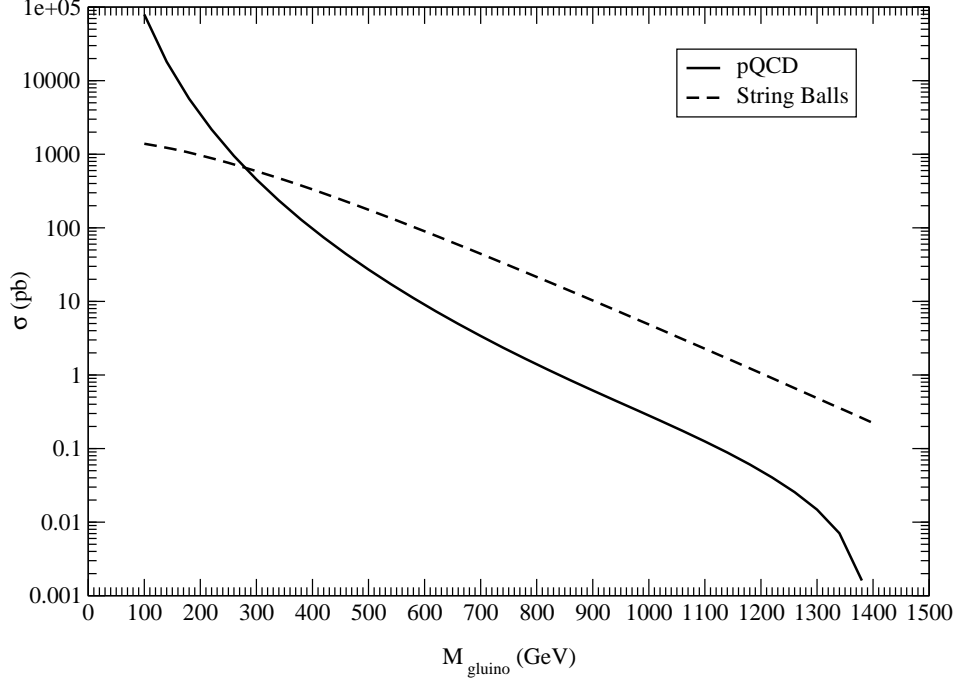


FIG. 3: Total cross section for gluino production at LHC as a function of gluino mass.

renormalization scales to be $Q = m_{\tilde{q}}, m_{\tilde{g}}$, (the squark and gluino masses respectively) and multiply a K factor of 1.5 to take into account the higher order corrections.

IV. SQUARK AND GLUINO PRODUCTION FROM TEV SCALE STRING BALLS AT LHC

The differential cross section for squark production with mass $M_{\tilde{q}}$, momentum \vec{p} and energy $E = \sqrt{\vec{p}^2 + M_{\tilde{q}}^2}$ from string ball of temperature T_{SB} at LHC is given by [35, 36]

$$\frac{E d\sigma_{\text{squark}}}{d^3p} = \frac{1}{(2\pi)^3 s} \sum_{ab} \int_{M_s^2}^{\frac{M_s^2}{g_s^4}} dM^2 \int \frac{dx_a}{x_a} f_{a/p}(x_a, \mu^2) f_{b/p}\left(\frac{M^2}{sx_a}, \mu^2\right) \hat{\sigma}^{ab}(M) \frac{A_n c_n \gamma \tau_{SB} p^\mu u_\mu}{(e^{\frac{p^\mu u_\mu}{T_{SB}}} - 1)}, \quad (20)$$

where M_s is the string mass scale and g_s is the string coupling which is less than 1 for the string perturbation theory to be valid, see eq. (1). The flow velocity is u^μ and γ is the Lorentz boost factor with

$$\gamma \vec{v}_{SB} = (0, 0, \frac{(x_1 - x_2)\sqrt{s}}{2M_{SB}}). \quad (21)$$

Squark Production From String Balls at LHC

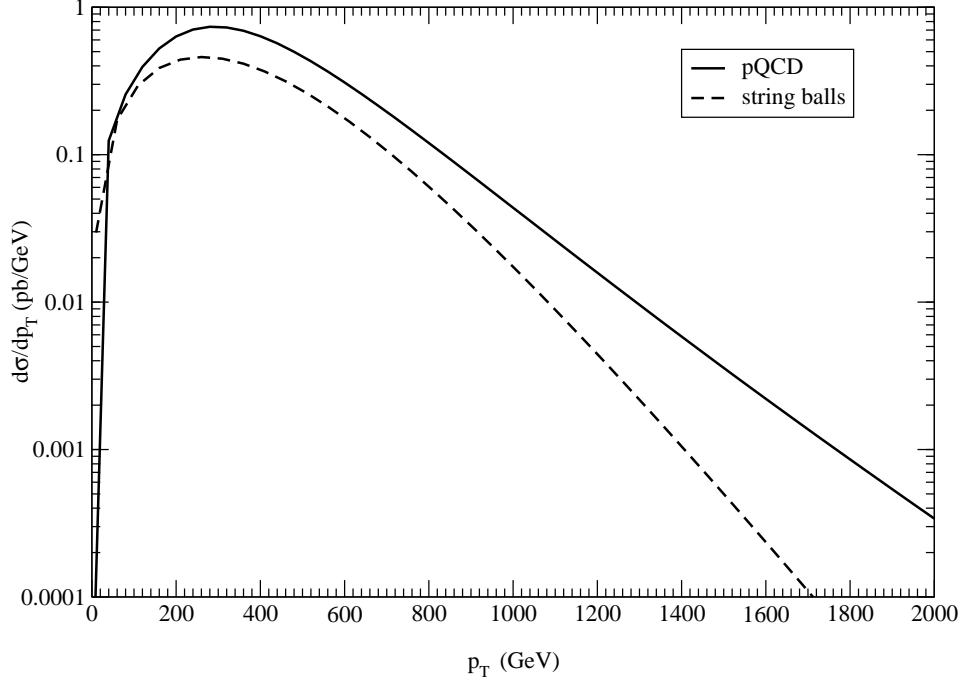


FIG. 4: p_T distribution of squark production at LHC.

A_n is the $d(=n+3)$ dimensional area factor [21, 36]. We will use the number of extra dimensions $n=6$ in our calculation. The partonic level string ball production cross section $\hat{\sigma}^{ab}$ is given by eq. (11). We have used CTEQ6M PDF [34] in our calculation.

Similarly, the differential cross section for gluino production with mass $M_{\tilde{g}}$, momentum \vec{p} and energy $E = \sqrt{\vec{p}^2 + M_{\tilde{g}}^2}$ from string ball of temperature T_{SB} at LHC is given by

$$\frac{E d\sigma_{\text{gluino}}}{d^3p} = \frac{1}{(2\pi)^3 s} \sum_{ab} \int_{M_s^2}^{\frac{M^2}{g_s^4}} dM^2 \int \frac{dx_a}{x_a} f_{a/p}(x_a, \mu^2) f_{b/p}\left(\frac{M^2}{sx_a}, \mu^2\right) \hat{\sigma}^{ab}(M) \frac{A_n c_n \gamma T_{SB} p^\mu u_\mu}{(e^{\frac{p^\mu u_\mu}{T_{SB}}} + 1)}. \quad (22)$$

V. RESULTS AND DISCUSSIONS

In this section we present the results of our calculation in pp collisions at LHC at $\sqrt{s} = 14$ TeV.

In Fig. 2 we contrast the result for squark production from the pQCD-SUSY calculation with that from thermal string ball emission as a function of squark mass in pp collisions at $\sqrt{s} = 14$ TeV at LHC. The solid line is squark production from the pQCD-SUSY calculation

Gluino Production From String Balls at LHC

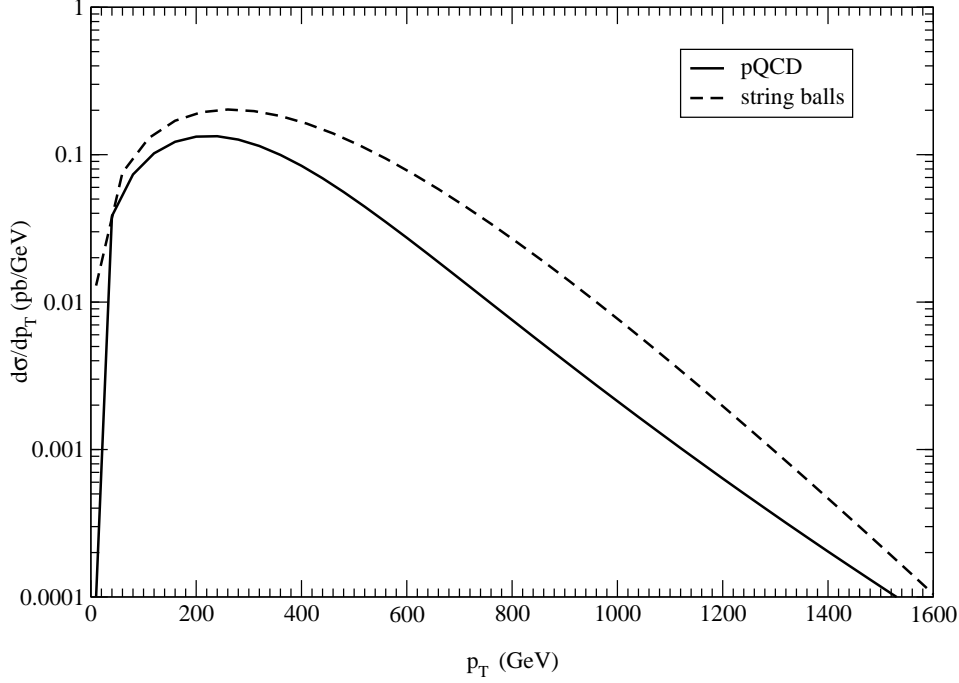


FIG. 5: p_T distribution of gluino production at LHC.

with $m_{\tilde{q}}/m_{\tilde{g}}=0.8$. The dashed line is squark production from string balls at with string mass scale $M_s = 1$ TeV. It can be seen that if the string mass scale $M_s \sim 1$ TeV then the squark production from string balls at LHC is much larger than that from pQCD-SUSY processes for squark mass larger than 200 GeV.

In Fig.3 we contrast the result for gluino production from the pQCD-SUSY calculation with that from thermal string ball emission as a function of gluino mass in pp collisions at $\sqrt{s} = 14$ TeV at LHC. The solid line is gluino production from the pQCD-SUSY calculation with $m_{\tilde{q}}/m_{\tilde{g}}=0.8$. The dashed line is gluino production from string balls with string mass scale $M_s = 1$ TeV. It can be seen that if the string mass scale $M_s \sim 1$ TeV then the gluino production from string balls at LHC is much larger than that from pQCD-SUSY processes for gluino mass larger than 300 GeV.

In Fig.4 we present $\frac{d\sigma}{dp_T}$ for the squark production cross section, both from pQCD-SUSY processes and from string balls at LHC. The solid line is the squark production cross section from direct pQCD-SUSY production processes as a function of p_T at LHC at $\sqrt{s} = 14$ TeV pp collisions. Here we have taken the squark mass to be 500 GeV with $m_{\tilde{q}}/m_{\tilde{g}} = 0.8$. The

Squark Production From String Balls at LHC

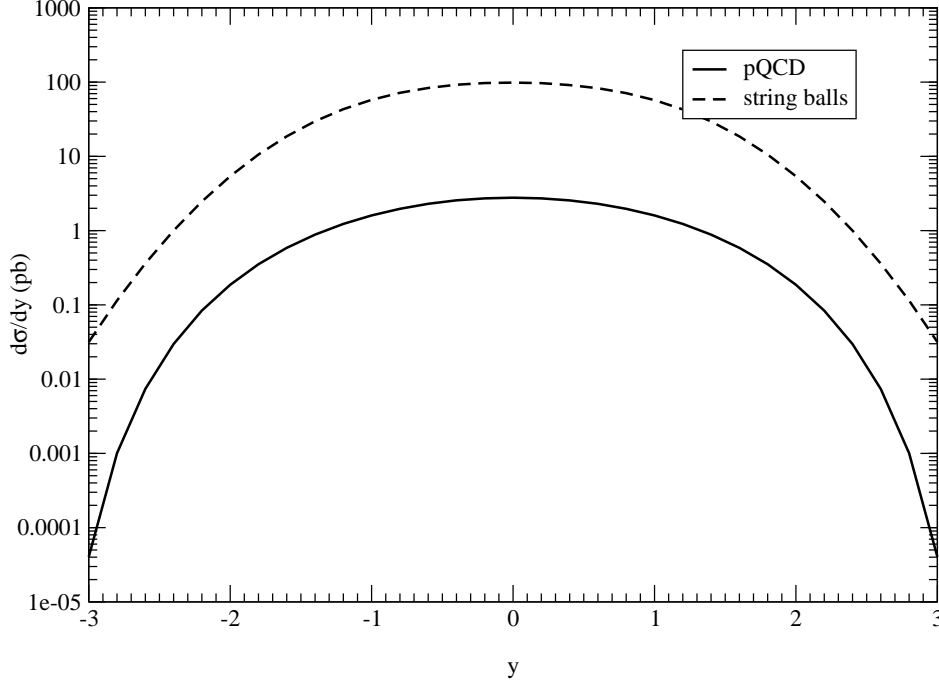


FIG. 6: Rapidity distribution of squark production at LHC.

dashed line is the p_T distribution of squark production from string balls with string mass scale $M_s = 1$ TeV.

In Fig.5 we present $\frac{d\sigma}{dp_T}$ for the gluino production cross section, both from pQCD-SUSY processes and from string balls at LHC. The solid line is the gluino production cross section from direct pQCD-SUSY production processes as a function of p_T at LHC at $\sqrt{s} = 14$ TeV pp collisions. Here we have taken the gluino mass to be 500 GeV with $m_{\tilde{q}}/m_{\tilde{g}} = 0.8$. The dashed line is the p_T distribution of gluino production from string balls with string mass scale $M_s = 1$ TeV.

In Fig.6 we present the rapidity distribution results for squark production both from pQCD-SUSY processes and from string balls at LHC. The solid line is the squark production cross section from direct pQCD-SUSY production processes as a function of rapidity at LHC at $\sqrt{s} = 14$ TeV pp collisions. Here we have taken squark mass to be 500 GeV with $m_{\tilde{q}}/m_{\tilde{g}} = 0.8$. The rapidity range covered is from -3 to 3. The dashed line is the rapidity distribution of squark production from string balls at LHC with string mass scale $M_s = 1$ TeV.

Gluino Production From String Balls at LHC

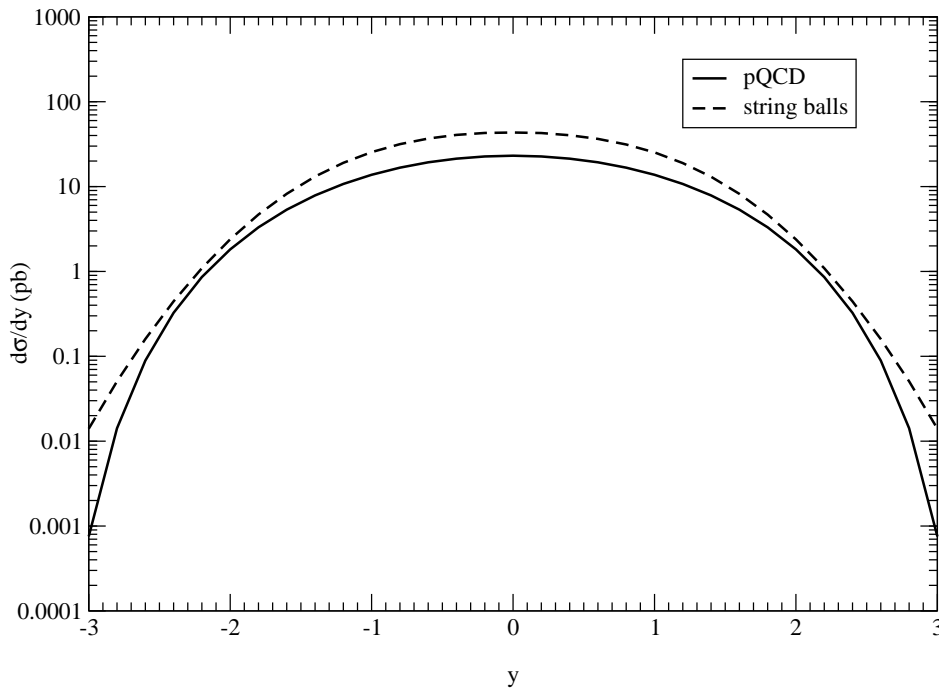


FIG. 7: Rapidity distribution of gluino production at LHC.

In Fig.7 we present the rapidity distribution results for gluino production both from pQCD-SUSY processes and from string balls at LHC. The solid line is the gluino production cross section from direct pQCD-SUSY production processes as a function of rapidity at LHC at $\sqrt{s} = 14$ TeV pp collisions. Here we have taken $m_{\tilde{q}}/m_{\tilde{g}} = 0.8$. The rapidity range covered is from -3 to 3. We have chosen the gluino mass to be 500 GeV. The dashed line is the rapidity distribution of gluino production from string balls at LHC with string mass scale $M_s = 1$ TeV.

From the above results it can be seen that there are significant squark and gluino production from string balls at LHC. Hence, in the absence of black hole production at LHC, an enhancement in the supersymmetry production may be a signature of TeV scale string physics at LHC.

VI. CONCLUSIONS

If extra dimensions are found in the second run of LHC in the pp collisions at $\sqrt{s} = 14$ TeV then the string scale can be \sim TeV, and we should produce string balls at LHC. In this

paper we have studied supersymmetry (squark and gluino) production from string balls at LHC in pp collisions at $\sqrt{s} = 14$ TeV and have compared that with the parton fusion results using pQCD. We have found significant squark and gluino production from string balls at LHC which is comparable to parton fusion pQCD results. Hence, in the absence of black hole production at LHC, an enhancement in supersymmetry production can be a signature of TeV scale string physics at LHC.

The LHC will also collide two lead nuclei at $\sqrt{s} = 5.5$ TeV per nucleon to produce quark-gluon plasma [2, 3, 37, 38]. Since the total energy in the two lead nuclei collisions at LHC will be ~ 1150 TeV, we may expect to see new physics [4] in the nuclear collisions at LHC as well.

-
- [1] ATLAS Collaboration, JHEP 1408 (2014) 103; Phys.Rev. D88 (2013) 7, 072001; Eur.Phys.J. C74 (2014) 12, 3134; Phys.Rev. D87 (2013) 1, 015010; New J.Phys. 15 (2013) 043007; JHEP 1304 (2013) 075; Phys.Rev.Lett. 110 (2013) 1, 011802; Phys.Lett. B710 (2012) 538; Eur.Phys.J. C75 (2015) 7, 318; JHEP 1409 (2014) 103; Phys.Rev. D90 (2014) 5, 052001; JHEP 1406 (2014) 035; Phys.Lett. B719 (2013) 261.
 - [2] M. Gyulassy and L. McLerran, Nucl. Phys. A750, 30 (2005), nucl-th/0405013; G. C. Nayak, A. Dumitru, L. McLerran and W. Greiner, Nucl. Phys. A687 (2001) 457; F. Cooper, E. Mottola and G. C. Nayak, Phys. Lett. B555 (2003) 181; R. S. Bhalerao and G. C. Nayak, Phys. Rev. C61 (2000) 054907; G. C. Nayak and V. Ravishankar, Phys. Rev. C58 (1998) 356; Phys. Rev. D55 (1997) 6877.
 - [3] F. Cooper and G. C. Nayak, Phys. Rev. D73 (2006) 065005; hep-th/0611125; hep-th/0612292; G. C. Nayak and R. Shrock, Phys.Rev. D77 (2008) 045008; G. C. Nayak, Eur. Phys. J.C59 (2009) 715; Int.J.Mod.Phys. A25 (2010) 1155; Eur.Phys.J. C59 (2009) 891; Electron.J.Theor.Phys. 8 (2011) 279; hep-th/0001009; Phys. Rev. D72 (2005) 125010.
 - [4] A. Chamblin, F. Cooper and G. C. Nayak, Phys. Rev. D69 (2004) 065010.
 - [5] N. Arkani-Hamed, S. Dimopoulos and G.R. Dvali, Phys. Lett. B429 (1998) 263; Phys. Rev. D59 (1999) 086004; I. Antoniadis, N. Arkani-Hamed, S. Dimopoulos and G.R. Dvali, Phys. Lett. B436 (1998) 257; L. Randall and R. Sundrum, Phys. Rev. Lett. 83 (1999) 3370; 83 (1999) 4690.

- [6] T. Banks and W. Fischler, hep-th/9906038.
- [7] S. Dimopoulos and G. Landsberg, Phys. Rev. Lett. 87 (2001) 161602; P.C. Argyres, S. Dimopoulos and J. March-Russell, Phys. Lett. B441 (1998) 96.
- [8] S. B. Giddings and S. Thomas, Phys. Rev. D65 (2002) 056010.
- [9] S. B. Giddings, in *Proc. of the APS/DPF/DPB Summer Study on the Future of Particle Physics (Snowmass 2001)* ed. R. Davidson and C. Quigg, hep-ph/0110127; M.B. Voloshin, Phys. Lett. B518 (2001) 137; Phys. Lett. B524 (2002) 376.
- [10] D. M. Eardley and S. B. Giddings, Phys. Rev. D66 (2002) 044011; S.N. Solodukhin, Phys. Lett. B533 (2002) 153; A. Jevicki and J. Thaler, Phys. Rev. D66 (2002) 024041.
- [11] L. Anchordoqui and H. Goldberg, Phys. Rev. D65 (2002) 047502; Phys. Rev. D67 (2003) 064010.
- [12] R. Casadio and B. Harms, Int. J. Mod. Phys. A17 (2002) 4635.
- [13] K. Cheung, Phys. Rev. D66 (2002) 036007; Phys. Rev. Lett. 88 (2002) 221602; K. Cheung and Chung-Hsien Chou, Phys. Rev. D66 (2002) 036008.
- [14] Y. Uehara, Mod. Phys. Lett. A17 (2002) 1551.
- [15] Seong Chan Park and H.S. Song, J. Korean Phys. Soc. 43 (2003) 30.
- [16] M. Bleicher, S. Hofmann, S. Hossenfelder and H. Stoecker, Phys. Lett. B548 (2002) 73; S. Hossenfelder, S. Hofmann, M. Bleicher and H. Stoecker, Phys. Rev. D66 (2002) 101502.
- [17] I. Mocioiu, Y. Nara and I. Sarcevic, Phys. Lett. B557 (2003) 87; V. Frolov and D. Stojkovic, Phys. Rev. D68 (2003) 064011; 67 (2003) 084004; 66 (2002) 084002; D. Ida and S. C. Park, Phys. Rev. D67 (2003) 064024; 69 (2004) 049901; B. Kol, hep-ph/0207037; M. Cavaglia, S. Das and R. Maartens, Class. Quant. Grav. 20 (2003) 1205; M. Cavaglia and S. Das, Class. Quant. Grav. 21 (2004) 4511; S. Hossenfelder, Phys. Lett. B598 (2004) 92; A. Ringwald, Fortsch. Phys. 51 (2003) 830.
- [18] T. Han, G. D. Kribs and B. McElrath, Phys. Rev. Lett. 90 (2003) 031601; P. Kanti, Int. J. Mod. Phys. A19 (2004) 4899; G. Landsberg, [arXiv: hep-ph/0211013]; M. Cavaglia, Int. J. Mod. Phys. A18 (2003) 1843; H. Stoecker, AIP Conf.Proc.947 (2007) 376; L. A. Anchordoqui, H. Goldberg and S. Nawata, arXiv:0804.2013 [hep-ph]; D-C. Dai, G. Starkman, D. Stojkovic, C. Issever, E. Rizvi and J. Tseng, Phys.Rev.D77 (2008) 076007.
- [19] A. Chamblin and G. C. Nayak, Phys. Rev. D66 (2002) 091901.
- [20] L. A. Anchordoqui, J. L. Feng, H. Goldberg and A. D. Shapere, Phys. Rev. D66 (2002) 103002;

- J. L. Feng and A. D. Shapere, Phys. Rev. Lett. 88 (2002) 021303; L. A. Anchordoqui, T. Paul, S. Reucroft and J. Swain, Int. J. Mod. Phys. A18 (2003) 2229; G. C. Nayak and J. Smith, Phys. Rev. D74 (2006) 014007; L. Anchordoqui and H. Goldberg, Phys. Rev. D67 (2003) 064010; G. C. Nayak, hep-ph/0211395; JHEP 1101 (2011) 039; A. Chamblin, F. Cooper and G. C. Nayak, Phys. Lett. B672 (2009) 147.
- [21] R. Emparan, M. Masip and R. Rattazzi, Phys. Rev. D65 (2002) 064023.
- [22] A. Ringwald and H. Tu, Phys. Lett. B525 (2002) 135.
- [23] A. Chamblin, S. W. Hawking and H. S. Reall, Phys. Rev. D61 (2000) 065007; R. Emparan, G. T. Horowitz and R. C. Myers, J. High Energy Phys. 01 (2000) 07.
- [24] S. Dimopoulos and R. Emparan, Phys. Lett. B526 (2002) 393, hep-ph/0108060.
- [25] M. Cavaglia and S. Das, Class. Quant. Grav. 21 (2004) 4511; M. Cavaglia, S. Das and R. Maartens, Class. Quant. Grav. 20 (2003) L205.
- [26] D. Baumann, P. Steinhardt and N. Turok, hep-th/0703250; S. Alexander and P. Meszaros, hep-th/0703070; P. Chen, New Astronomy Reviews 49 (2005) 233; Nucl. Phys. B (Proc. Suppl.) 124 (2003) 103.
- [27] G. C. Nayak, Phys.Part.Nucl.Lett. 8 (2011) 337.
- [28] L. Susskind, hep-th/9309145.
- [29] M. J. Bowick, L. Smolin and L. C. Wijewardhana, Phys. Rev. Lett. 56 (1986) 424; E. Halyo, B. Kol, A. Rajaraman and L. Susskind, Phys. Lett. B 401 (1997) 15; G. Veneziano, in *NATO Advanced Study Workshop on Hot Hadronic Matter: Theory and Experiment*, Divonne-les-Bains, France, 27 Jun-1 jul 1994; G. T. Horowitz and J. Polchinski, Phys. Rev. D55 (1997) 6189; Phys. Rev. D57 (1998) 2557; T. Damour G. Veneziano, Nucl. Phys. B568 (2000) 93.
- [30] D. Amati and J. G. Russo, Phys. Lett. B454 (1999) 207, hep-th/9901092.
- [31] D. M. Gingrich and K. Martell, Phys. Rev. D78 (2008) 115009, arXiv:0808.2512 [hep-ph].
- [32] A. Chamblin, F. Cooper and G. C. Nayak, Phys.Rev.D70 (2004) 075018.
- [33] W. Beenakker *et al.*, Nucl. Phys. B492 (1997) 51.
- [34] J. Pumplin, *et al.*, JHEP 0207 (2002) 102.
- [35] A. E. Erkoca, G. C. Nayak and I. Sarcevic, Phys. Rev. D79 (2009) 094011.
- [36] G. C. Nayak, JHEP 0906 (2009) 071.
- [37] F. Cooper, C-W. Kao and G. C. Nayak, Phys.Rev. D66 (2002) 114016; D. Dietrich, G. C. Nayak and W. Greiner, Phys.Rev. D64 (2001) 074006; J.Phys. G28 (2002) 2001;

- hep-ph/0009178; J. Ruppert, G. C. Nayak, D. Dietrich, H. Stoecker and W. Greiner, Phys.Lett. B520 (2001) 233; Q. Wang, C-W. Kao, G. C. Nayak, H. Stoecker and W. Greiner, Int.J.Mod.Phys. E10 (2001) 483.
- [38] G. C. Nayak and P. van Nieuwenhuizen, Phys. Rev. D71 (2005) 125001; M. C. Birse, C-W. Kao and G. C. Nayak, Phys.Lett. B570 (2003) 171; C-W. Kao, G. C. Nayak and W. Greiner, Phys.Rev. D66 (2002) 034017; G. C. Nayak, Phys.Lett. B442 (1998) 427; JHEP 9802 (1998) 005.